IEEE Photonics Journal
An IEEE Photonics Society Publication

Open Access

Stokes Space Representation of Modal Dispersion

Volume 9, Number 5, October 2017

Ioannis Roudas, ***Member, IEEE***
Jaroslaw Kwapisz

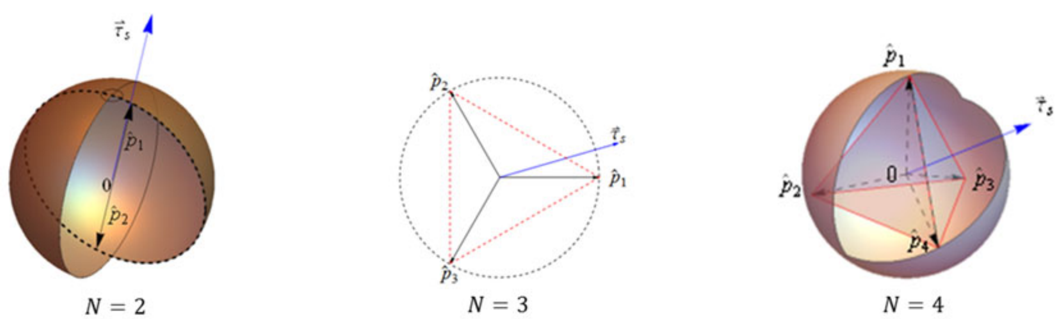

Generalized Stokes representation of the principal modes $\hat{p}_i$, $i = 1, \ldots, N$ and the input modal dispersion vector $\vec{\tau}_s$ for a *N*-mode fiber

DOI: 10.1109/JPHOT.2017.2735403
1943-0655 © 2017 IEEE

Stokes Space Representation of Modal Dispersion

Ioannis Roudas,[1] ***Member, IEEE***, **and Jaroslaw Kwapisz**[2]

[1]Electrical and Computer Engineering, Montana State University, Bozeman, MT 59717 USA
[2]Mathematical Sciences, Montana State University, Bozeman, MT 59717 USA

DOI:10.1109/JPHOT.2017.2735403

Manuscript received July 19, 2017; accepted July 29, 2017. Date of publication August 3, 2017; date of current version August 29, 2017. Corresponding author: Ioannis Roudas (e-mail: ioannis.roudas@montana.edu).

Abstract: Polarization-mode dispersion in single-mode fibers can be viewed as a special case of modal dispersion in multimode and multicore optical fibers. Exploiting the similarity between these two transmission effects, modal dispersion can be modeled in a way analogous to that of polarization-mode dispersion by modifying the conventional Jones–Stokes formalism. In this paper, we review the geometrical representation of modal dispersion in the generalized Stokes space by means of the modal dispersion vector. We summarize and unify the fundamental equations that encapsulate the properties of the modal dispersion vector. We prove that the modal dispersion vector can be expressed as a linear superposition of the Stokes vectors representing the principal modes. The coefficients of this expansion are the corresponding differential mode group delays. This concise and elegant expression can be considered as a simplified definition of the modal dispersion vector and can be used to facilitate analytical calculations.

Index Terms: Optical fiber communication, multimode optical fiber, multicore optical fiber, modal dispersion, spatial division multiplexing.

1. Introduction

The available capacity of the installed fiber-optic backbone network infrastructure will be rapidly depleted as the compound annual growth rate (CAGR) of global data crossing the Internet is expected to exceed 20% in the years to come [1], [2]. To accommodate this traffic increase, several variants of spatial division multiplexing (SDM) are currently considered. A fiber-thrifty SDM solution may be implemented by using different modes of multimode optical fibers (MMFs) or different cores of multicore optical fibers (MCFs) to increase the spectral efficiency of congested links [3], [4]. Whether this approach can lead to potential cost savings in the future compared to other alternative SDM methods is still a subject of debate.

Linear transmission impairments in MMFs and MCFs include, among others, modal dispersion (MD), mode-dependent loss (MDL), multipath interference, and intermodal/intercore crosstalk [5]. This paper is devoted to accurately modeling MD in MMFs and MCFs in the absence of all other modal effects. Under these conditions, MD may be viewed as a generalization of polarization-mode dispersion (PMD) in single-mode fibers (SMFs) [5]. The similarities between MD and PMD led to the extension of the PMD formalism, expressed in the conventional Jones and Stokes spaces [6]–[10], into higher dimensions [11]–[19]. In this mathematical framework, MD in N-mode MMFs/N-core MCFs can be fully described in a generalized N-dimensional Jones space by a set of orthogonal propagation modes called principal modes (PMs) and their corresponding differential

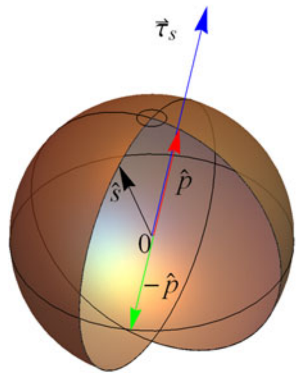

Fig. 1. Poincaré sphere, input slow and fast PSPs, $\hat{p}$ and $-\hat{p}$, respectively, and input PMD vector $\vec{\tau}_s$ in the case of SMF ($N = 2$). An arbitrary launch state of polarization (SOP) is denoted by $\hat{s}$.

mode group delays (DMGDs) with respect to the average group delay [5]. Alternatively, MD can be geometrically represented by a vector (called the MD vector) in a generalized Stokes space with $N^2 - 1$ dimensions [11].

To the best of our knowledge, no explicit analytical relationship has existed among the MD vector, the PMs, and DMGDs. In this paper, we show for the first time that the MD vector can be expressed as a weighted sum of the Stokes vectors representing the PMs, with the corresponding DMGDs as coefficients. This leads to a new definition of the MD vector that encapsulates both the PMs and the DMGDs into a single mathematical expression.

The rest of the paper is organized as follows: In Section II, we review the generalized Jones and Stokes formalism [11]–[19] for the modeling of MD in MMFs and MCFs. More specifically, we take a brief look in the generalized Jones vectors and matrices, the expansion of the latter in terms of the generalized Gell-Mann matrices, the transition between the generalized Jones and Stokes spaces using the above expansion, and the properties of the vector dot products in both spaces. In Section III, we derive a concise analytical relationship that links the MD vector with the input PMs and the corresponding DMGDs. The details of the formalism are discussed in the Appendices.

2. Theoretical Background

2.1 Literature Survey and Motivation

The modification of the PMD formalism for the modeling of MD in long-haul SDM optical communications systems began circa 2005, with Fan and Kahn [20] who showed that the concept of principal states of polarization (PSPs) in SMFs [6] could be generalized to the PMs in MMFs/MCFs. Subsequently, Ho and Kahn [5] used a random unitary matrix concatenation model to derive analytical expressions for the probability density functions (pdf's) of the DMDGs and the MDL in the strong coupling regime. Antonelli *et al.* [11] extended Gordon and Kogelnik's spinor PMD formalism [9] to the modeling of MD in MMFs/MCFs and introduced the MD vector for the Stokes space representation of MD. In addition, they derived analytical expressions for the pdf of the MD vector modulus and two autocorrelation functions related to the MD vector in the case of strongly-coupled MMFs/MCFs. Several follow-up papers, e.g., [12]–[19], elucidated various facets of this formalism.

The aim of this paper is twofold: (i) To review the MD formalism and reconcile the differences in the mathematical conventions adopted by various authors [11]–[19]; (ii) To derive a new analytical relationship linking the MD vector to the PMs and their corresponding DMGDs.

The MD vector is a generalization of the PMD vector for $N > 2$, where N is the number of spatial and polarization modes. Recall the conventional definition of the input PMD vector $\vec{\tau}_s$ as the product of the slow input PSP vector $\hat{p}$ in Stokes space and the differential group delay (DGD) τ between the two PSPs (Fig. 1) [9].

It is also possible to redefine the input PMD vector $\vec{\tau}_s$ as the sum of the Stokes vectors representing the slow and fast PSPs, $\hat{p}$ and $-\hat{p}$, respectively, scaled by the corresponding DGDs $\tau/2$, $-\tau/2$ with respect to the average group delay. This new definition yields a PMD vector identical to the conventional one

$$\vec{\tau}_s \triangleq \frac{\tau}{2}\hat{p} + \left(-\frac{\tau}{2}\right)(-\hat{p}) = \tau\hat{p}. \tag{1}$$

The advantage of this new definition is that it can be generalized in the case of higher dimensions $N > 2$, whereas the conventional definition of the PMD vector fails to scale with the number of modes.

We will show in Section III that, in all cases ($N \geq 2$), the input MD vector $\vec{\tau}_s$ can be written as a weighted sum of the Stokes vectors $\hat{p}_i$, representing the input PMs, with the corresponding DMGDs (with respect to the average group delay) τ_i, $i = 1, \ldots, N$ as coefficients [see expression (22) below].

2.2 Generalized Jones and Stokes Spaces

In the following, we use the methodology and the notation of [9], [10]: Dirac's bra-ket vectors represent unit vectors in the generalized Jones space and hats represent unit vectors in the generalized Stokes space.

The phasor of the electric field of a monochromatic optical wave at a given position **r** in an N-mode waveguide can be expressed as the vector sum

$$\mathbf{E}(\mathbf{r}) = \sum_{k=1}^{N} c_k \mathbf{E}_k(\mathbf{r}), \tag{2}$$

where $\mathbf{E}_k(\mathbf{r})$ represent the electric field phasors of individual modes and the complex coefficients c_k, $k = 1, \ldots, N$ are the mode excitations [11]. The latter satisfy the relationship

$$\sum_{k=1}^{N} |c_k|^2 = 1. \tag{3}$$

We define the generalized unit Jones vectors as $|s\rangle \triangleq [c_1, \ldots, c_N]^T$, where T denotes the transpose of a matrix. Combinations of propagation modes are described by such vectors.

Linear optical devices are represented by $N \times N$ complex matrices called generalized Jones matrices, similar to the two-dimensional case. Their action results in a simple multiplication of the input Jones vector by the corresponding Jones matrix.

Traditionally, the Stokes space representation of polarization is useful for visualizing and solving optics problems without resorting to complex algebraic calculations based on Jones matrix concatenation. For instance, we can gain considerable physical insight from the pictorial representation of the polarization evolution during propagation though optical devices in terms of rotations in Stokes space.

The generalized Stokes formalism allows the depiction of a combination of N modes in a $(N^2 - 1)$-dimensional Stokes space as a point on the surface of a $(N^2 - 2)$-hypersphere (i.e., a generalized Poincaré sphere) with unit radius [11]–[19]. The Stokes space can also be used for the representation of MD in a concise form in terms of the MD vector [11]–[19].

The above geometrical representation of MD is less intuitive than its polarization counterpart due to the high-dimensionality of the generalized Stokes space, although it does have aesthetic appeal. The question then arises whether there are any advantages at all in using the generalized Stokes space instead of the generalized Jones space for $N > 2$.

The primary advantage of this modeling approach is that several mathematical properties of PMD can be generalized for MD and can be expressed in a concise and elegant fashion using equations evolving Stokes space vectors [11]–[19]. For instance, the DMGD of narrowband optical pulses during propagation in MMFs/MCFs can be written simply as the inner product of the input MD vector and the Stokes vector corresponding to the launched combination of modes [19] [see expression (21) below]. Based on this relationship, it is possible to measure the MD of MMFs/MCFs using the mode-dependent signal delay method [19].

We can move to the Stokes space representation using the fact that any matrix in the N-dimensional Jones space can be expressed as a linear combination of N^2 base matrices. Here, without loss of generality, we use as basis the $N \times N$ identity matrix $\mathbf{I}$ and the $N^2 - 1$ generalized Gell-Mann matrices $\boldsymbol{\Lambda}_1, \ldots, \boldsymbol{\Lambda}_{N^2-1}$ with dimensions $N \times N$ [22], [23]. The latter can be constructed as follows: Consider an arbitrary orthonormal basis in Jones space $|b_1\rangle, \ldots, |b_N\rangle$. We first define the following auxiliary symmetric, antisymmetric, and diagonal matrices, respectively [22], [23]:

$$\mathbf{U}_{jk} \triangleq |b_j\rangle\langle b_k| + |b_k\rangle\langle b_j|, \tag{4}$$

$$\mathbf{V}_{jk} \triangleq -i\left(|b_j\rangle\langle b_k| - |b_k\rangle\langle b_j|\right), \tag{5}$$

$$\mathbf{W}_l \triangleq \sqrt{\frac{2}{l(l+1)}}\left(\sum_{j=1}^{l} |b_j\rangle\langle b_j| - l|b_{l+1}\rangle\langle b_{l+1}|\right), \tag{6}$$

for given indices j, k, l.

Then, we define the sets [22], [23]

$$\begin{aligned}
\mathcal{U} &\triangleq \{\mathbf{U}_{jk} : 1 \le j < k \le N\},\\
\mathcal{V} &\triangleq \{\mathbf{V}_{jk} : 1 \le j < k \le N\},\\
\mathcal{W} &\triangleq \{\mathbf{W}_l : 1 \le l \le N-1\}.
\end{aligned} \tag{7}$$

The generalized Gell-Mann matrices $\boldsymbol{\Lambda}_i$ are the elements of the union of the above sets, i.e., $\boldsymbol{\Lambda}_i \in \mathcal{U} \cup \mathcal{V} \cup \mathcal{W},\ i = 1, \ldots, N^2 - 1$ [22], [23]. The order in which the elements $\boldsymbol{\Lambda}_i$ are listed is immaterial since reordering them results in a permutation of the Stokes vector components in (12).

From their definition, we note that the generalized Gell-Mann matrices are traceless and mutually trace-orthogonal [22], [23]

$$\begin{aligned}
&\mathrm{Tr}\left(\boldsymbol{\Lambda}_i\right) = 0,\\
&\mathrm{Tr}\left(\boldsymbol{\Lambda}_i\boldsymbol{\Lambda}_j\right) = 2\delta_{ij},
\end{aligned} \tag{8}$$

where Tr(.) denotes the trace operator and δ_{ij}, $i, j = 1, \ldots, N^2 - 1$, denotes the Kronecker delta.

To express concisely a Jones matrix as a linear combination of the identity matrix and the $N^2 - 1$ generalized Gell-Mann matrices, we also need to define the Gell-Mann vector $\boldsymbol{\Lambda} \triangleq [\boldsymbol{\Lambda}_1, \ldots, \boldsymbol{\Lambda}_{N^2-1}]^T$, in analogy to the Pauli spin vector [9].

To illustrate the expansion of a Jones matrix in terms of the identity matrix and the $N^2 - 1$ generalized Gell-Mann matrices, following the methodology of [9], we first define the dyadic operator $|p\rangle\langle q|$ as the outer product of two generalized Jones vectors $|p\rangle = [p_1, \ldots, p_N]^T$, $|q\rangle = [q_1, \ldots, q_N]^T$

$$\Xi \triangleq |p\rangle\langle q| = \begin{bmatrix} p_1 q_1^* & p_1 q_2^* & \cdots & p_1 q_N^* \\ p_2 q_1^* & p_2 q_2^* & \cdots & p_2 q_N^* \\ \vdots & \vdots & \ddots & \vdots \\ p_N q_1^* & p_N q_2^* & \cdots & p_N q_N^* \end{bmatrix}, \tag{9}$$

where the asterisk denotes the complex conjugate.

A special case of a dyadic operator is the projection operator, which represents a mode filter, i.e., the equivalent of a polarizer in the two-dimensional case

$$\rho \triangleq |s\rangle \langle s| = \begin{bmatrix} |c_1|^2 & c_1 c_2{}^* & \cdots & c_1 c_N{}^* \\ c_2 c_1{}^* & |c_2|^2 & \cdots & c_2 c_N{}^* \\ \vdots & \vdots & \ddots & \vdots \\ c_N c_1{}^* & c_N c_2{}^* & \cdots & |c_N|^2 \end{bmatrix}. \tag{10}$$

By using (4)–(8), we write the projection operator as a sum of the identity matrix and the $N^2 - 1$ generalized Gell-Mann matrices $\{\mathbf{I}, \mathbf{\Lambda}_1, \ldots, \mathbf{\Lambda}_{N^2-1}\}$ [12], [17] (see Appendix A)

$$|s\rangle \langle s| = \frac{1}{N}\left[\mathbf{I} + \sqrt{\frac{N(N-1)}{2}}\hat{s} \cdot \mathbf{\Lambda}\right], \tag{11}$$

where we defined the generalized Stokes vectors as [12], [17]

$$\hat{s} \triangleq \sqrt{\frac{N}{2(N-1)}} \langle s| \mathbf{\Lambda} |s\rangle . \tag{12}$$

The normalization coefficients in (11), (12) are chosen such that $\|\hat{s}\| = 1$ (cf. Appendix A).

It should be emphasized that Antonelli *et al.* [11] used different multiplication coefficients for (11), (12) due to their different definition of the generalized Gell-Mann matrices, of the trace-orthogonality relationship, and due to the adoption of non-unit Stokes vectors for $N > 2$ (see expression (9) and the Appendix in [11]). In contrast, our choice of (4)–(8) and unit Stokes vectors (12) complies with [12], [13], [17], and [22]. Both approaches are backwards compatible with the PMD case [9], [10] ($N = 2$).

One can use the following eigenvalue equation as an inverse transform from Stokes to Jones space [10]

$$(\hat{s} \cdot \mathbf{\Lambda})\, |s\rangle = \sqrt{\frac{2(N-1)}{N}}\, |s\rangle . \tag{13}$$

Equation (13) stems from the expansion of the projection operator (10) in terms of the identity matrix and the $N^2 - 1$ Gell-Mann matrices (11). This is done by multiplying (11) with $|s\rangle$ from the right and rearranging the terms. Expression (13) indicates that the Jones vector $|s\rangle$ corresponding to the Stokes vector $\hat{s}$ is the eigenvector of the operator $(\hat{s} \cdot \mathbf{\Lambda})$ corresponding to the $\sqrt{2(N-1)/N}$ eigenvalue. Most points on the generalized Poincaré sphere do not satisfy (13), which means that they do not correspond to valid combinations of modes (see Fig. 4(a)–(d) and the discussion in Appendix B).

The dot products of two vectors in Jones and Stokes spaces are connected by the following equation [11], [22]:

$$|\langle q \mid p \rangle|^2 = \frac{1}{N}\left[1 + (N - 1)\, \hat{p} \cdot \hat{q}\right]. \tag{14}$$

To obtain (14), we first write the dyadic operator (9) as a linear combination of the identity matrix and the $N^2 - 1$ Gell-Mann matrices and then we multiply with $|p\rangle$ from the right and $\langle q|$ from the left.

Orthogonal vectors in Jones space correspond to non-orthogonal vectors in Stokes space. Setting $\langle q \mid p \rangle = 0$ in (14), we obtain [22]

$$\hat{p} \cdot \hat{q} = -\frac{1}{N - 1}. \tag{15}$$

The dot product property (15) is satisfied by the N vectors connecting the origin of the axes with the N vertices of a $(N-1)$-dimensional regular simplex centered at the origin and inscribed in the unit $N^2 - 2$-dimensional Poincaré sphere [22]. Conversely, this indicates that the N vectors of an

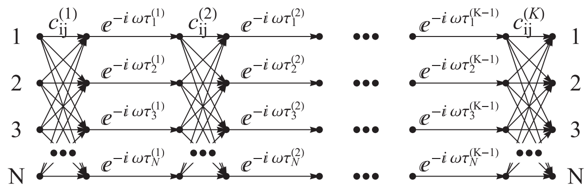

Fig. 2. Trellis diagram visualization of the simulation model of a long MMF/MCF link with N modes/cores composed of a concatenation of $K - 1$ uncoupled short uniform fiber segments with K coupling stages in between. All functionalities can be implemented using $N \times N$ unitary matrices in Jones space [5]. (Symbols: Nodes = fiber modes, $\tau_i^{(k-1)}$ = DMGD of the i-th mode in the k-th segment, $c_{i,j}^{(k)}$ = coupling coefficient between the i-th and the j-th modes in the k-th segment).

orthonormal basis in Jones space are mapped into Stokes vectors which form the vertices of such $(N - 1)$-dimensional regular simplex [22] (cf. Fig. 3).

In Appendix B, we illustrate the above generalized Jones-Stokes formalism for the case of a hypothetical trimodal waveguide.

2.3 Modeling of Modal Dispersion in Long MMFs/MCFs

A long linear MMF/MCF link can be modeled as a concatenation of independent short fiber segments [5]. The latter can be implemented using random unitary matrices for the coupling sections and diagonal unitary matrices for the delay sections (Fig. 2).

From the directed graph shown in Fig. 2, we can write the following matrix equation that connects the input $|s\rangle$ and output $|t(\omega)\rangle$ Jones vectors [9]

$$|t(\omega)\rangle = \mathbf{U}(\omega)\,|s\rangle\,, \tag{16}$$

where $\mathbf{U}(\omega)$ is the unitary transfer matrix of the fiber in Jones space.

The input PMs are the eigenstates of the operator [9]

$$i\mathbf{U}(\omega)^{\dagger}\mathbf{U}_{\omega}(\omega)|p_i(\omega)\rangle \triangleq \tau_i(\omega)|p_i(\omega)\rangle, \tag{17}$$

where $\tau_i(\omega)$, $i = 1, \ldots, N$, are the corresponding DMGDs.

In (17), the average mode group delay is assumed zero for convenience [11]

$$\sum_{i=1}^{N} \tau_i(\omega) = 0. \tag{18}$$

The input MD vector $\vec{\tau}_s$ is defined as

$$i\mathbf{U}(\omega)^{\dagger}\mathbf{U}_{\omega}(\omega) \triangleq \sqrt{\frac{N-1}{2N}}\vec{\tau}_s(\omega)\cdot\mathbf{\Lambda}, \tag{19}$$

where the index ω denotes differentiation with respect to the angular frequency and $\dagger$ denotes the adjoint matrix.

The j-th component of the input MD vector is given by

$$[\vec{\tau}_s(\omega)]_j = \sqrt{\frac{N}{2(N-1)}}\mathrm{Tr}\left[i\mathbf{U}(\omega)^{\dagger}\mathbf{U}_{\omega}(\omega)\mathbf{\Lambda}_j\right]. \tag{20}$$

It is worth pointing out that Antonelli *et al.* [11], Hu *et al.* [12], and Milione *et al.* [19] each used a different multiplication coefficient in the RHS of (19), which results in a different scaling of the input MD vector. All these choices are legitimate since (19) constitutes the defining equation of $\vec{\tau}_s$. The rationale behind our convention was to use for consistency the same multiplication coefficient in front of $\hat{s}$ and $\vec{\tau}_s$ in (11) and (19), respectively.

Finally, it has been shown by Millione *et al.* [19] that the group delay τ_g of an optical pulse corresponding to a given combination of launch modes is related to the dot product of the input MD vector $\vec{\tau}_s(\omega)$ and the input launch state $\hat{s}$ in Stokes space. We rewrite their expression in a slightly modified form:

$$\tau_g = \frac{N-1}{N}\langle\vec{\tau}_s(\omega)\rangle\cdot\hat{s}, \tag{21}$$

where angle brackets denote spectral averaging [9].

It is worth noting that (21) differs from the original expression (16) of Millione *et al.* [19] on several points: there is a corrective multiplicative factor of $(N-1)/N$, the input MD vector $\vec{\tau}_s$ is spectrally-averaged, and the average mode group delay is set to zero according to (18). The above changes are necessary in order to make (21) compatible with (11), (12) and with expression [5.30] in [9].

3. Modal Dispersion Vector

We will show that, in the absence of MDL, the input MD vector can be written as a weighted sum of the Stokes vectors representing the input PMs with the corresponding DMGDs as coefficients

$$\boxed{\vec{\tau}_s(\omega) = \sum_{i=1}^{N}\tau_i(\omega)\,\hat{p}_i(\omega)\,.} \tag{22}$$

Since the input and output PMs form orthonormal bases in Jones space, according to (15), they are mapped into Stokes vectors that form the vertices of $(N-1)$-dimensional regular simplices. It is possible to visualize these simplices in the case of bimodal fibers ($N=2$) (i.e., the PSPs $\hat{p}$, $-\hat{p}$ form a straight line in Fig. 1), as well as in the case of hypothetical trimodal ($N=3$) and quadrimodal ($N=4$) waveguides (Fig. 3), where the PMs form an equilateral triangle and a regular tetrahedron, respectively. In general, the Stokes vector in the direction of the MD vector does not coincide with a state that corresponds to a valid combination of modes in Jones space, i.e., the eigenvalue (13) is not satisfied (cf. Appendix D).

To prove (22), we first express the group delay operator $i\mathbf{U}(\omega)^{\dagger}\mathbf{U}_{\omega}(\omega)$ using its spectral decomposition in terms of its eigenvalues $\tau_i(\omega)$ and eigenvectors $|p_i(\omega)\rangle$, $i=1,\ldots,N$

$$i\mathbf{U}(\omega)^{\dagger}\mathbf{U}_{\omega}(\omega) = \sum_{k=1}^{N}\tau_k(\omega)|p_k(\omega)\rangle\langle p_k(\omega)|. \tag{23}$$

In addition, the projection operators $|p_k(\omega)\rangle\langle p_k(\omega)|$ can be written according to (11) as

$$|p_k(\omega)\rangle\langle p_k(\omega)| = \frac{1}{N}\left[\mathbf{I} + \sqrt{\frac{N(N-1)}{2}}\hat{p}_k(\omega)\cdot\mathbf{\Lambda}\right]. \tag{24}$$

By substitution of (24) into (23) and taking into account that the average mode group delay is assumed zero (18), we obtain

$$i\mathbf{U}(\omega)^{\dagger}\mathbf{U}_{\omega}(\omega) = \sqrt{\frac{N-1}{2N}}\sum_{k=1}^{N}\tau_k(\omega)\hat{p}_k(\omega)\cdot\mathbf{\Lambda}. \tag{25}$$

Comparison of the RHS of expressions (19), (25) yields the desired expression (22). Q.E.D.

The practical value of (22) is illustrated in Appendices C-D. In Appendix C, we rederive previously known analytical expressions for the norm of the MD vector and the projections of the MD vector on the PMs. In Appendix D, we show that the MD vector points along a unit vector $\hat{n}$ in Stokes space that is not related, in general, to any valid combination of input modes in Jones space for $N>2$.

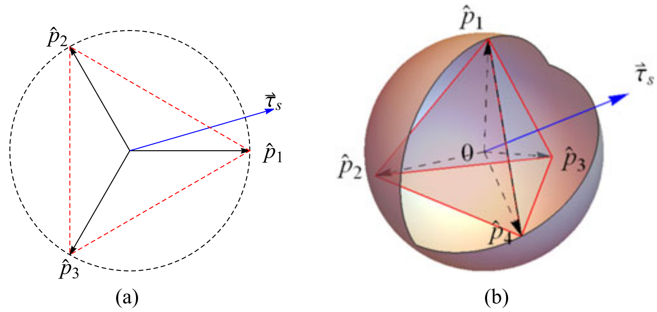

Fig. 3. (a) For a hypothetical trimodal waveguide, the Stokes space is eight dimensional. The input PMs in Stokes space are vectors from the origin of the axes to the vertices of an equilateral triangle. The input MD vector is on the same plane as the input PMs. The dotted circle indicates the boundaries of the generalized Poincaré sphere. (b) For a hypothetical quadrimodal waveguide, the Stokes space is 15-dimensional. The input PMs in Stokes space are vectors from the origin of the axes to the vertices of a regular tetrahedron. The input MD vector lies in the same 3D subspace as the input PMs. To delineate the edges of the regular tetrahedron, we inscribed it in a sphere of unit radius which is the intersection of the generalized Poincaré sphere with the 3D subspace.

4. Concluding Remarks

There is currently no consensus regarding the most appropriate mathematical conventions for the Stokes representation of MD in order to facilitate analytical calculations. We performed a brief survey of the main articles [11]–[19] on the topic of the generalized Jones and Stokes spaces and identified several apparent differences regarding the definitions of fundamental quantities, e.g., the Stokes vectors and the MD vector, adopted by various authors. The initial motivation for this article was to reconcile these differences in the generalized Stokes formalism in the exclusive presence of MD. Therefore, we compiled the most important analytical expressions derived in the previous literature and reformulated them using our own preferred mathematical conventions. By doing so, we identified a fundamental property of the MD vector that has not been previously recognized, i.e., we highlighted the fact that the MD vector can be written as a linear superposition of the PMs, using the DMGDs as coefficients. This simple and elegant expression can be used to gain physical insight and facilitate analytical calculations. As a first example of its practical value, in Appendix C, we rederived previously known expressions for the length and the projections of the MD vector on the PMs using vector properties in Stokes space, without transitioning between Jones and Stokes spaces. Then, in Appendix D, we tackled a particularly interesting question that has not been addressed before, namely, the conditions under which the MD vector can have a direction in Stokes space that corresponds to a valid combination of modes in Jones space. Again, we showed that our new definition of the MD vector in terms of the PMs and the DMGDs allows to solve this problem in a straightforward manner. Finally, in Appendix B, we illustrated the use of our unified Stokes formalism by studying the case of a trimodal waveguide.

Appendix

A. Projection Matrix Expansion

In this Appendix, we provide a detailed derivation of the projection matrix expansion in terms of the identity matrix and the $N^2 - 1$ Gell-Mann matrices and justify the use of normalization coefficients in (11), (12).

We express the projection matrix as a linear combination of the identity matrix and the $N^2 - 1$ Gell-Mann matrices (11)

$$|s\rangle \langle s| = \alpha \mathbf{I} + \beta \hat{s} \cdot \mathbf{\Lambda}, \tag{26}$$

where α, β are unknown normalization coefficients (to be determined) and $\hat{s}$ is the unit Stokes vector corresponding to the unit Jones vector $|s\rangle$ (to be defined below).

We will use the identities [11]

$$\mathrm{Tr}\left[|s\rangle\langle s|\right] = \langle s|s\rangle = 1, \tag{27}$$

$$\mathrm{Tr}(\mathbf{I}) = N. \tag{28}$$

Taking the trace of (26) and substituting (27), (28) yields

$$\alpha = 1/N. \tag{29}$$

Multiplying (26) with $\mathbf{\Lambda}_j$ from the right and taking the trace yields

$$[\hat{s}]_j = \frac{1}{2\beta}\,\langle s|\mathbf{\Lambda}_j|s\rangle, \tag{30}$$

or, equivalently,

$$\hat{s} = \frac{1}{2\beta}\langle s|\mathbf{\Lambda}|s\rangle. \tag{31}$$

To determine β, we will use the identity [11]

$$\mathrm{Tr}\left[(\hat{s}\cdot\mathbf{\Lambda})^2\right] = 2\|\hat{s}\|^2 = 2. \tag{32}$$

Solving (26) for $\hat{s}\cdot\mathbf{\Lambda}$ and squaring yields

$$(\hat{s}\cdot\mathbf{\Lambda})^2 = \frac{1}{\beta^2}\left[(1-2\alpha)\,|s\rangle\,\langle s| + \alpha^2\mathbf{I}\right]. \tag{33}$$

Taking the trace of both hands of (33) and substituting the value of α from (29) yields

$$\beta = \sqrt{\frac{N-1}{2N}}. \tag{34}$$

B. Modal Dispersion of Trimodal Waveguides

This Appendix is dedicated to the mathematical description of three-mode linear propagation using the generalized Jones-Stokes formalism. In reality, the total number of spatial and polarization modes of circularly-symmetric, multimode fibers is always an even number. Nevertheless, the hypothetical trimodal waveguide can be used as an example in order to illustrate the formalism of Section II. In addition, one can profit from extensive studies of qutrits in quantum mechanics and the correspondence between three-dimensional Hilbert space vectors and eight-dimensional Bloch vectors, e.g., [24]–[27].

Based on the discussion in Section II-B, we define the generalized unit Jones vectors in Cartesian coordinates as

$$|s\rangle = [c_1, c_2, c_3]^T = \left[c_{01}e^{j\varphi_1}, c_{02}e^{j\varphi_2}, c_{03}e^{j\varphi_3}\right]^T, \tag{35}$$

where c_{0k} are the magnitudes and φ_k are the phases of c_k, $k = 1, \ldots, 3$.

We can parametrize the magnitudes $c_{0k}, k = 1, \ldots, 3$ using spherical coordinates $c_{01} = \cos\phi\sin\theta$, $c_{02} = \sin\phi\sin\theta$, $c_{03} = \cos\theta$. We assume that the angular spherical coordinates θ, ϕ take values in the interval $[0, \pi/2)$ so that the magnitudes c_{0k}, $k = 1, \ldots, 3$ are always positive.

Any two Jones vectors differing by a complex multiplicative factor are physically equivalent, i.e., they represent the same physical state [22]. Therefore, we can take $e^{j\varphi_3}$ out of the parenthesis in (35) as a common factor, and define $\chi = \varphi_1 - \varphi_3$, $\psi = \varphi_2 - \varphi_3$. The phases $\chi, \psi \in [0, 2\pi)$ so that the electric fields of the three modes can take both positive and negative values. Thus, we can then rewrite (35) in polar form

$$|s\rangle = \left[e^{j\chi}\cos\phi\sin\theta, e^{j\psi}\sin\phi\sin\theta, \cos\theta\right]^T. \tag{36}$$

TABLE 1
Gell-Mann Matrices in the Standard Basis

$\mathbf{\Lambda}_1 = \begin{pmatrix} 0 & 1 & 0 \\ 1 & 0 & 0 \\ 0 & 0 & 0 \end{pmatrix}$	$\mathbf{\Lambda}_2 = \begin{pmatrix} 0 & -i & 0 \\ i & 0 & 0 \\ 0 & 0 & 0 \end{pmatrix}$	$\mathbf{\Lambda}_3 = \begin{pmatrix} 1 & 0 & 0 \\ 0 & -1 & 0 \\ 0 & 0 & 0 \end{pmatrix}$
$\mathbf{\Lambda}_4 = \begin{pmatrix} 0 & 0 & 1 \\ 0 & 0 & 0 \\ 1 & 0 & 0 \end{pmatrix}$	$\mathbf{\Lambda}_5 = \begin{pmatrix} 0 & 0 & -i \\ 0 & 0 & 0 \\ i & 0 & 0 \end{pmatrix}$	$\mathbf{\Lambda}_6 = \begin{pmatrix} 0 & 0 & 0 \\ 0 & 0 & 1 \\ 0 & 1 & 0 \end{pmatrix}$
$\mathbf{\Lambda}_7 = \begin{pmatrix} 0 & 0 & 0 \\ 0 & 0 & -i \\ 0 & i & 0 \end{pmatrix}$	$\mathbf{\Lambda}_8 = \frac{1}{\sqrt{3}}\begin{pmatrix} 1 & 0 & 0 \\ 0 & 1 & 0 \\ 0 & 0 & -2 \end{pmatrix}$	

TABLE 2
Stokes Vector Calculated From a Jones Vector Expressed in Cartesian and Polar Forms

Cartesian form	Polar form
$\hat{s} = \frac{\sqrt{3}}{2}\begin{bmatrix} c_1c_2{}^* + c_2c_1{}^* \\ i\,(c_1c_2{}^* - c_2c_1{}^*) \\ \lvert c_1\rvert^2 - \lvert c_2\rvert^2 \\ c_1c_3{}^* + c_3c_1{}^* \\ i\,(c_1c_3{}^* - c_3c_1{}^*) \\ c_2c_3{}^* + c_3c_2{}^* \\ i\,(c_2c_3{}^* - c_3c_2{}^*) \\ \frac{1}{\sqrt{3}}\left(\lvert c_1\rvert^2 + \lvert c_2\rvert^2 - 2\lvert c_3\rvert^2\right) \end{bmatrix}$	$\hat{s} = \frac{\sqrt{3}}{2}\begin{bmatrix} \sin^2\theta \sin(2\phi)\cos(\chi-\psi) \\ -\sin^2\theta \sin(2\phi)\sin(\chi-\psi) \\ \sin^2\theta \cos(2\phi) \\ 2\sin\theta\cos\theta\cos\phi\cos\chi \\ -2\sin\theta\cos\theta\cos\phi\sin\chi \\ 2\sin\theta\cos\theta\sin\phi\cos\psi \\ -2\sin\theta\cos\theta\sin\phi\sin\psi \\ -\frac{1}{2\sqrt{3}}\left[3\cos(2\theta)+1\right] \end{bmatrix}$

It is worth noting that an arbitrary Jones vector depends on four real parameters. This means that the corresponding Stokes vector obtained below by (38) belongs to a four-dimensional manifold in the 8D Stokes space [17].

The expressions of the Gell-Mann matrices in the standard basis $|1\rangle, |2\rangle, |3\rangle$ are given by (4)–(6) after reordering

$$\begin{aligned} &\mathbf{\Lambda}_1 = |1\rangle\langle 2| + |2\rangle\langle 1| && \mathbf{\Lambda}_5 = -i\,(|1\rangle\langle 3| - |3\rangle\langle 1|) \\ &\mathbf{\Lambda}_2 = -i\,(|1\rangle\langle 2| - |2\rangle\langle 1|) && \mathbf{\Lambda}_6 = |2\rangle\langle 3| + |3\rangle\langle 2| \\ &\mathbf{\Lambda}_3 = |1\rangle\langle 1| - |2\rangle\langle 2| && \mathbf{\Lambda}_7 = -i\,(|2\rangle\langle 3| - |3\rangle\langle 2|) \\ &\mathbf{\Lambda}_4 = |1\rangle\langle 3| + |3\rangle\langle 1| && \mathbf{\Lambda}_8 = \frac{1}{\sqrt{3}}\,(|1\rangle\langle 1| + |2\rangle\langle 2| - 2\,|3\rangle\langle 3|) \end{aligned} \tag{37}$$

Substituting $|1\rangle = [1, 0, 0]^T$, $|2\rangle = [0, 1, 0]^T$, $|3\rangle = [0, 0, 1]^T$, we obtain the familiar expressions shown in Table 1 [22].

From the definition of the generalized Stokes vectors (12), we have

$$\hat{s} \triangleq \frac{\sqrt{3}}{2}\,\langle s|\,\mathbf{\Lambda}\,|s\rangle \tag{38}$$

By substituting (35), (36) into (38), we can derive the explicit form of the Stokes vector $\hat{s}$ corresponding to the Jones vector $|s\rangle$ in Cartesian and polar coordinates (Table 2).

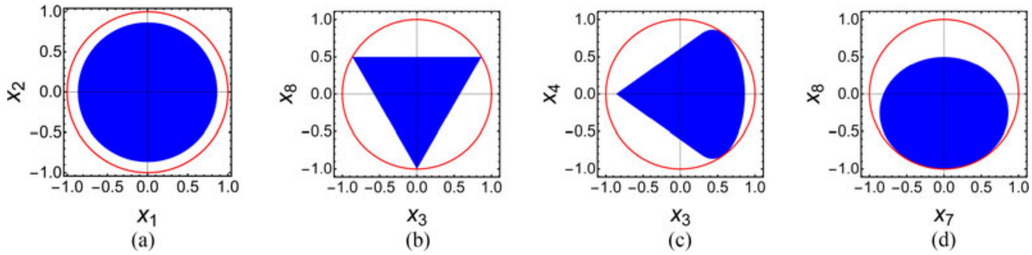

Fig. 4. Projections of the valid states on the Poincaré 7-sphere on four different planes defined by pairs of Stokes axes $\{x_i, x_j\}$ (a) $\{x_1, x_2\}$. (b) $\{x_3, x_8\}$. (c) $\{x_3, x_4\}$. (d) $\{x_7, x_8\}$. The red circles indicate the boundaries of the generalized Poincaré sphere.

Notice the similarity of the eight-dimensional Stokes vector in the left column of Table 2 with the conventional 3D Stokes vector [9]

$$\hat{s} = \left[|c_1|^2 - |c_2|^2, c_1 c_2{}^* + c_2 c_1{}^*, i\left(c_1 c_2{}^* - c_2 c_1{}^*\right)\right]^T. \tag{39}$$

The first three elements are identical apart from a multiplication factor and a cyclic permutation of the components. Actually, all the information of the eight-dimensional Stokes vector can be recast into three conventional 3D Stokes vectors corresponding to the combinations $\{c_1, c_2\}, \{c_1, c_3\}, \{c_2, c_3\}$ of the Jones vector components. This suggests a possible visual representation by three interdependent points on three interrelated 3D Poincaré spheres. A similar approach was proposed in quantum mechanics for the multi-Bloch vector representation of the qutrit [24].

From (13), we obtain the following relationship as the inverse transform between Stokes and Jones vectors

$$(\hat{s} \cdot \mathbf{\Lambda})\,|s\rangle = \frac{2}{\sqrt{3}}\,|s\rangle \tag{40}$$

By substituting the polar form of the Stokes vector from the right column of Table 2 into (40), we find that the eigenvalues of the operator $\frac{\sqrt{3}}{2}(\hat{s} \cdot \mathbf{\Lambda})$ are 1, $-1/2$, $-1/2$ independent of the values of the four angles θ, ϕ, χ, ψ. This can be used as a test in order to verify whether a given Stokes vector corresponds to a valid combination of propagation modes or not.

The vast majority of points on the Poincaré 7-sphere do not satisfy (40), which means that they do not correspond to valid combinations of propagation modes. This can be illustrated by plotting the projection of the valid states on the surface of the Poincaré 7-sphere onto various planes defined by different pairs of Stokes axes $\{x_i, x_j\}$ (Fig. 4(a)–(d)). The blue areas in the region plots in Fig. 4(a)–(d) are calculated by using the corresponding components of the Stokes vector on the right column of Table 2. If the valid states covered the entire Poincaré sphere, their projections onto any plane would completely fill the unit circle (in red). As we can see in the Fig. 4(a)–(d), this is never the case. We conclude that there are unutilized areas on the surface of the generalized Poincaré sphere (see also several papers in quantum mechanics [25]–[27] that studied the shape of the boundaries of the regions on the Bloch sphere that contain valid states).

C. Norm and Projections of the MD Vector on the PMs

In this Appendix, we will use our definition of the input MD vector (22) to prove the MD vector properties given by the relationships (41) and (42) below. These expressions were initially derived by Antonelli *et al.* [11] using a different method. Here, they differ slightly from their original form in [11] due to our choice of multiplication coefficients in (11), (12), and (19).

More specifically, we will show that:

1) The norm of the input MD vector $\vec{\tau}_s(\omega)$ is given by

$$\|\vec{\tau}_s(\omega)\| = \sqrt{\frac{N}{N-1}\sum_{k=1}^{N}\tau_k^2(\omega)}. \tag{41}$$

2) The input MD vector $\vec{\tau}_s(\omega)$ is not aligned to any particular input PM $\hat{p}_{s,i}$. Its projection on the input PMs is given by

$$\vec{\tau}_s(\omega)\cdot\hat{p}_i(\omega) = \frac{N}{N-1}\tau_i(\omega), \tag{42}$$

where $i = 1, \ldots, N$.

We will first prove relationship (41). Squaring both sides of (22) yields

$$\begin{aligned}\|\vec{\tau}_s(\omega)\|^2 &= \sum_{i=1}^{N}\sum_{j=1}^{N}\tau_i(\omega)\,\tau_j(\omega)\,\hat{p}_i(\omega)\cdot\hat{p}_j(\omega)\\ &= \sum_{i=1}^{N}\tau_i^2(\omega) + 2\sum_{i=1}^{N}\sum_{j=i+1}^{N}\tau_i(\omega)\,\tau_j(\omega)\,\hat{p}_i(\omega)\cdot\hat{p}_j(\omega).\end{aligned}$$

On substituting (15) we obtain

$$\|\vec{\tau}_s(\omega)\|^2 = \sum_{i=1}^{N}\tau_i^2(\omega) - \frac{2}{N-1}\sum_{i=1}^{N}\sum_{j=i+1}^{N}\tau_i(\omega)\,\tau_j(\omega). \tag{43}$$

By squaring (18), the result is

$$2\sum_{i=1}^{N}\sum_{j=i+1}^{N}\tau_i(\omega)\,\tau_j(\omega) = -\sum_{i=1}^{N}\tau_i^2(\omega). \tag{44}$$

By substituting (44) into (43), we obtain

$$\|\vec{\tau}_s(\omega)\|^2 = \frac{N}{N-1}\sum_{i=1}^{N}\tau_i^2(\omega),$$

and thus (41) is proved by taking the positive square root of both sides.

Q.E.D.

Next, we will use our definition of the input MD vector (22) to prove relationship (42). First, we multiply both sides of (22) with $\hat{p}_i$

$$\vec{\tau}_s(\omega)\cdot\hat{p}_i(\omega) = \sum_{j=1}^{N}\tau_j(\omega)\,\hat{p}_j(\omega)\cdot\hat{p}_i(\omega). \tag{45}$$

By substituting (15) into (45), we get

$$\vec{\tau}_s(\omega)\cdot\hat{p}_i(\omega) = \tau_i(\omega) - \frac{1}{N-1}\sum_{j\neq i}^{N}\tau_j(\omega). \tag{46}$$

Rearranging the terms in (18) yields

$$\sum_{j\neq i}^{N}\tau_j(\omega) = -\tau_i(\omega). \tag{47}$$

By substituting (47) into (46), we obtain the desired expression (42).

Q.E.D.

D. Additional MD Vector Properties

In this Appendix, we discuss the conditions under which the direction of the input MD vector corresponds to a valid combination of input modes in Jones space for $N > 2$.

As a starting point, we write the unit vector $\hat{n}$ along the direction of the input MD vector in Stokes space as $\hat{n} = \vec{\tau}_s/\tau$, where τ denotes the norm $\|\vec{\tau}_s\|$ of the MD vector as given by (41). From the definition of the input MD vector (19), we obtain:

$$(\hat{n} \cdot \mathbf{\Lambda}) = \frac{1}{\tau}\sqrt{\frac{2N}{N - 1}} i\mathbf{U}^{\dagger}(\omega)\,\mathbf{U}_{\omega}(\omega)\,. \tag{48}$$

From (17), the eigenvectors and eigenvalues of the group delay operator $i\mathbf{U}^{\dagger}(\omega)\,\mathbf{U}_{\omega}(\omega)$ are $|p_i\rangle, \tau_i, i = 1, \ldots, N$. Assume that one of the above eigenvectors, say $|p_j\rangle$, satisfies the inverse Jones-Stokes transform (13)

$$(\hat{n} \cdot \mathbf{\Lambda})\,|p_j\rangle = \sqrt{\frac{2\,(N - 1)}{N}}\,|p_j\rangle. \tag{49}$$

Then, the remaining $N - 1$ eigenvectors of the group delay operator satisfy the eigenvalue equation [11]

$$(\hat{n} \cdot \mathbf{\Lambda})\,|p_i\rangle = -\sqrt{\frac{2}{N\,(N - 1)}}\,|p_i\rangle\,, i = 1, \ldots, N, i \neq j. \tag{50}$$

Combining (48)–(50), we conclude that the DMGDs must assume the following values

$$\tau_j = \frac{N}{N - 1}\tau, \tag{51}$$

$$\tau_i = -\frac{1}{N}\tau, i = 1, \ldots, N, i \neq j. \tag{52}$$

Alternatively, it is straightforward to obtain the above result using our definition of the MD vector (22) and the Stokes vector properties (15), (42). Since $|p_j\rangle$ satisfies (49), then $\vec{\tau}_s = \tau\hat{p}_j$. Consequently, we can write the inner products $\vec{\tau}_s \cdot \hat{p}_j$, $\vec{\tau}_s \cdot \hat{p}_i$ in terms of the length of the MD vector τ as $\vec{\tau}_s \cdot \hat{p}_j = \tau$, $\vec{\tau}_s \cdot \hat{p}_i = \tau\hat{p}_j \cdot \hat{p}_i = -\tau/(N - 1)$, the latter expression obtained by using (15). In addition, independent of the orientation of the input MD vector, the inner product $\vec{\tau}_s \cdot \hat{p}_i$ is always related to the individual DMGDs based on (42). Combining these results, we obtain immediately (51), (52).

Conversely, using a counterexample, we will show that when (51), (52) are not satisfied, i.e., when the input MD vector is not aligned with an eigenvector $\hat{p}_i, i = 1, \ldots, N$, of the group delay operator its direction is not related to any valid combination of input modes in Jones space for $N > 2$.

For simplicity, consider the diagonal fiber transfer matrix for $N = 3$

$$\mathbf{U}(\omega) = \begin{bmatrix} e^{-i\omega\tau_1} & 0 & 0 \\ 0 & e^{-i\omega\tau_2} & 0 \\ 0 & 0 & e^{-i\omega\tau_3} \end{bmatrix}. \tag{53}$$

Solving the 3×3 system of equations (19) using (20) yields

$$\vec{\tau}_s = \frac{\sqrt{3}}{2}\,(\tau_1 - \tau_2)\,\hat{x}_3 + \frac{3}{2}\,(\tau_1 + \tau_2)\,\hat{x}_8, \tag{54}$$

where $\hat{x}_i$, $i = 1, ..., 8$ are the unit Stokes vectors along the Stokes axes.

Next, without loss of generality, assume that $\tau_1 = -\tau_2 = T$. In this specific case, the unit vector $\hat{n}$ in Stokes space along the direction of the MD vector is $\hat{n} = \vec{\tau}_s/\|\vec{\tau}_s\| = \hat{x}_3$. For the unit vector $\hat{n}$ in Stokes space to correspond to a valid combination of input modes in Jones space, (40) must be satisfied. Since $\hat{n} \cdot \mathbf{\Lambda} = \mathbf{\Lambda}_3$, we have to check whether $\mathbf{\Lambda}_3$ has an eigenvalue equal to $2/\sqrt{3}$. The eigenvectors of $\mathbf{\Lambda}_3$ are $|1\rangle$, $|2\rangle$, $|3\rangle$ with eigenvalues $1, -1, 0$, respectively. Therefore, we conclude that the direction of $\hat{n}$ does not correspond to a valid combination of input modes. The same conclusion can be drawn by inspection of Fig. 4(b).

A final observation is that the matrix $\mathbf{U}(\omega)$ does not represent a rotation around an axis along the direction of the MD vector for $N > 2$.

For instance, for the above special case, we obtain

$$\mathbf{U}(\omega) = \frac{1}{3}(1 + 2\cos\omega T)\mathbf{I} - i\sin\omega T\,\boldsymbol{\Lambda}_3 + \frac{1}{\sqrt{3}}(\cos\omega T - 1)\boldsymbol{\Lambda}_8. \tag{55}$$

which is obviously unrelated to $\vec{\tau}_s = \sqrt{3}T\hat{x}_3$.

Acknowledgment

The authors would like to thank D. Nolan, W. A. Wood, J. Yang, and T. A. Nguyen of Corning for fruitful discussions and K. Hetke of Montana State University for proofreading the original manuscript and for providing editorial assistance. The authors would also like to thank the anonymous reviewers for their comments and suggestions that improved the quality of the manuscript.

References

[1] P. J. Winzer and D. T. Neilson, “From scaling disparities to integrated parallelism: A decathlon for a decade,” *J. Lightw. Technol.*, vol. 35, no. 5, pp. 1099–1115, Mar. 2017.
[2] Cisco, Cisco Global Cloud Index: Forecast and Methodology, 2015–2020, Cisco, San Jose, CA, USA, 2016.
[3] D. Richardson, J. Fini, and L. Nelson, “Space-division multiplexing in optical fibres,” *Nature Photon.*, vol. 7, pp. 354–362, 2013.
[4] D. J. Richardson, “New optical fibres for high-capacity optical communications,” *Philos. Trans. Roy. Soc. A*, vol. 374, no. 2062, 2016, doi: 10.1098/rsta.2014.0441.
[5] K.-P. Ho and J. M. Kahn, “Mode coupling and its impact on spatially multiplexed systems,” in *Optical Fiber Telecommunications VIB*. San Diego, CA, USA: Academic, 2013, pp. 491–568.
[6] C. D. Poole and R. E. Wagner, “Phenomenological approach to polarisation dispersion in long single-mode fibres,” *Electron. Lett.*, vol. 22, pp. 1029–1030, 1986.
[7] C. D. Poole and J. Nagel, “Polarization effects in lightwave systems,” in *Optical Fiber Telecommunications IIIA*. San Diego, CA, USA: Academic, 1997, pp. 114–161.
[8] H. Kogelnik, L. E. Nelson, and R. M. Jopson, “Polarization mode dispersion,” in *Optical Fiber Telecommunications IVB*, I. P. Kaminow, T. Li, Eds. San Diego, CA, USA: Academic, 2002.
[9] J. P. Gordon and H. Kogelnik, “PMD fundamentals: Polarization mode dispersion in optical fibers,” *Proc. Nat. Acad. Sci. USA*, vol. 97, pp. 4541–4550, 2000.
[10] J. N. Damask, *Polarization Optics in Telecommunications*. New York, NY, USA: Springer, 2004.
[11] C. Antonelli, A. Mecozzi, M. Shtaif, and P. J. Winzer, “Stokes-space analysis of modal dispersion in fibers with multiple mode transmission,” *Opt. Exp.*, vol. 20, pp. 11718–11733, 2012.
[12] Q. Hu and W. Shieh, “Autocorrelation function of channel matrix in few-mode fibers with strong mode coupling,” *Opt. Exp.*, vol. 21, pp. 22153–22165, 2013.
[13] Q. Hu, X. Chen, A. Li, and W. Shieh, “High-dimensional Stokes-space analysis for monitoring fast change of mode dispersion in few-mode fibers,” in *Proc. Opt. Fiber Commun. Conf. (OFC)*, San Francisco, CA, USA, 2014, Paper W3D.3.
[14] G. Li, N. Bai, N. Zhao, and G. Xia, “Space-division multiplexing: The next frontier in optical communication,” *Adv. Opt. Photon.*, vol. 6, pp. 413–487, 2014.
[15] C. Antonelli, A. Mecozzi, and M. Shtaif, “The delay spread in fibers for SDM transmission: Dependence on fiber parameters and perturbations,” *Opt. Exp.*, vol. 23, pp. 2196–2202, 2015.
[16] S. Ö. Arik, K.-P. Ho, and J. M. Kahn, “Delay spread reduction in mode-division multiplexing: Mode coupling versus delay compensation,” *J. Lightw. Technol.*, vol. 33, no. 21, pp. 4504–4512, Nov. 2015.
[17] W. A. Wood, W. Miller, and M. Mlejnek, “A geometrical perspective on the coherent multimode optical field and mode coupling equations,” *IEEE J. Quantum Electron.*, vol. 51, no. 7, Jul. 2015, Art. no. 6100206.
[18] A. Mecozzi, C. Antonelli, and M. Shtaif, “Intensity impulse response of SDM links,” *Opt. Exp.*, vol. 23, pp. 5738–5743, 2015.
[19] G. Milione, D. A. Nolan, and R. R. Alfano, “Determining principal modes in a multimode optical fiber using the mode dependent signal delay method,” *J. Opt. Soc. Amer. B*, vol. 32, pp. 143–149, Jan. 2015.
[20] S. Fan and J. M. Kahn, “Principal modes in multimode waveguides,” *Opt. Lett.*, vol 30, pp. 135–137, 2005.
[21] S. Huard, *Polarization of light*. New York, NY, USA: Wiley, 1997.
[22] D. Aerts and M. Sassoli de Bianchi, “The extended Bloch representation of quantum mechanics and the hidden-measurement solution to the measurement problem,” *Ann. Phys.*, vol. 351, pp. 975–1025, 2014.
[23] R. A. Bertlmann and P. Krammer, “Bloch vectors for qudits,” *J. Phys. A*, vol. 41, 2008, Art. no. 235303.
[24] P. Kurzyński, “Multi-Bloch vector representation of the qutrit,” *Quantum Inf. Comput.*, vol. 11, pp. 361–373, 2011.

[25] S. K. Goyal, B. N. Simon, R. Singh, and S. Simon, "Geometry of the generalized Bloch sphere for qutrits," *J. Phys. A, Math. Theor.*, vol. 49, 2016, Art. no. 165203.
[26] G. Sarbicki and I. Bengtsson, "Dissecting the qutrit," *J. Phys. A, Math Theor.*, vol. 46, 2013, Art. no. 035306.
[27] I. P. Mendaš, "The classification of three-parameter density matrices for a qutrit," *J. Phys. A, Math. Gen.*, vol. 39, pp. 11313–11324, 2006.